A VARIATIONAL APPROACH TO JPEG ANTI-FORENSICS

Wei Fan [*,†], *Kai Wang* [*], *François Cayre* [*], *and Zhang Xiong* [†]

[*]GIPSA-Lab, CNRS UMR5216, 11 rue des Mathématiques, F-38402 St-Martin d'Hères Cedex, France
[†]School of Computer Science and Engineering, Beihang University, Beijing 100191, P. R. China

ABSTRACT

The objective of JPEG anti-forensics is to remove all the possible footprints left by JPEG compression. By contrary, there exist detectors that attempt to identify any telltale of the image tampering operation of JPEG compression and JPEG anti-forensic processing. This paper makes contribution on improving the undetectability of JPEG anti-forensics, with a higher visual quality of processed images. The employment of constrained total variation based minimization for deblocking successfully fools the forensic methods detecting JPEG blocking, and another advanced JPEG forensic detector. Calibration-based detector is also defeated by conducting a further feature value optimization. Experimental results show that the proposed method outperforms the state-of-the-art methods in a better trade-off between forensic undetectability and visual quality of processed images.

Index Terms— Digital image forensics, anti-forensics, JPEG compression, total variation, subgradient method

1. INTRODUCTION

Increasing development of high-quality cameras and powerful photo-editing tools significantly reduces the difficulty to make visually plausible fake images. Doctored images are appearing with growing frequency, for instance, in advertising and in political and personal attacking. Doubts of the authenticity have been thrown upon digital images. Image forensics has enjoyed its popularity to restore some trust, as it serves as a passive and blind authentication technique without any *a priori* embedded information compared to digital watermarking. Anti-forensics can help researchers study the weaknesses in existing forensic techniques for further development of trustworthy digital forensics.

In this paper, we concentrate on image anti-forensics that disguises the footprints of JPEG compression. In order to conceal the JPEG compression history of digital images, which can be detected by [1], Stamm et al. [2] recently proposed a DCT histogram smoothing method to fill the gaps in the comb-like distribution of DCT coefficients in each subband. For fooling another blocking artifact detector in [1], Stamm et al. later proposed to carry out a deblocking operation [3] after the DCT histogram smoothing.

The JPEG anti-forensic processing in [2] leaves footprints which can be detected by two advanced detectors [4, 5]. Its another disadvantage is to noticeably degrade the image visual quality [6, 4]. The first contribution of this paper, is to formulize the anti-forensic JPEG deblocking as a total variation (TV) based variational image restoration problem, which can be solved using subgradient method. The new deblocking method allows us to achieve a better visual quality of the anti-forensic image; meanwhile the blocking artifact detectors and a TV-based detector [4] are successfully fooled. The second contribution of this paper, is to defeat the calibration-based detector in [5], by directly optimizing the feature value after the previous deblocking process.

The remainder of this paper is organized as follows. Sec. 2 reviews related work on forensics, anti-forensics and countering anti-forensics of JPEG compressed images. The proposed JPEG TV-based deblocking method is described in Sec. 3. Sec. 4 presents the optimization problem against Lai and Böhme's calibration-based detector [5]. Sec. 5 shows some experimental results. Finally, we provide some discussions and draw conclusions in Sec. 6.

The first author performed this work while at GIPSA-Lab on the grant from China Scholarship Council (No. 2011602067). This work was also funded, in part, by French ANR Estampille (No. ANR-10-CORD-019).

2. RELATED WORK

During JPEG compression (here we refrain from repeating the standard JPEG compression process), two known artifacts appear, indicating the JPEG compression history of one image. The first one is the *quantization artifacts* in *DCT domain*. The DCT coefficients are clustered around the integer multiples of the quantization step length, leaving a comb-like distribution of DCT coefficients in each subband. The second one is the *blocking artifacts* in *spatial domain*. There are consistent discontinuities across block borders. Both of them are traces left from an image's JPEG compression history.

2.1. Detecting JPEG compression

Fan and De Queiroz [1] proposed an algorithm for maximum-likelihood estimation (MLE) of the JPEG quantization table, from a spatial-domain bitmap representation of the image. The method can also serve as a detector to classify an image as not JPEG compressed, if all the entries of the estimated quantization table are either 1 or "undetermined" [1, 2].

Fan and De Queiroz [1] also proposed a JPEG blocking signature measure as:

$$K_F = \sum_n |H_I(n) - H_{II}(n)|, \tag{1}$$

where $H_I(n)$ and $H_{II}(n)$ are normalized histograms of pixel differences across block boundaries and within the block, respectively.

2.2. JPEG anti-forensics

In order to disguise the quantization artifacts, Stamm et al. [2] proposed to add a dithering signal d to the DCT coefficient z in each subband:

$$z_d = z + d, \tag{2}$$

so that the dithered signal z_d approximates the distribution of the unquantized coefficients. For AC components, d is distributed in

such a way that z_d approximately follows a Laplacian distribution; for the DC component, d follows a uniform distribution. The adding of d succeeds in fooling the MLE of the quantization table in [1].

After the dithering operation, Stamm et al. [3] later proposed an anti-forensic deblocking operation against the blocking artifact detector of Fan and De Queiroz [1], that is the blocking signature measure K_F of Eq. (1). For each pixel at location (i, j), the anti-forensically deblocked image pixel value is obtained according to:

$$y_{i,j} = \text{med}_s(x_{i,j}) + w_{i,j}, \tag{3}$$

where $x_{i,j}$ is the original pixel value, $\text{med}_s(\cdot)$ is the median filtering operation with window size s, and $w_{i,j}$ is a low-power white Gaussian noise of variance σ^2.

2.3. Countering JPEG anti-forensics

Valenzise et al. [6, 4] claimed that the dithering signal [2] degraded the image quality. A forgery detector is therefore designed by measuring the noisiness of the re-compressed image, employing the TV of the image (the ℓ_1 norm of the spatial first-order derivatives) [7]. For a given image, the detector re-compresses it using different quality factors q, as a function of which, $\text{TV}(q)$ is computed. The backward finite difference quotient $\text{TV}^{(h)}(q)$ with lag h is calculated as:

$$\text{TV}^{(h)}(q) = \frac{1}{h}(\text{TV}(q) - \text{TV}(q-h)). \tag{4}$$

The forensic measure is:

$$K_V^h = \max(\text{TV}^{(h)}(q)). \tag{5}$$

Lai and Böhme [5] proposed another calibration-based detector to counter Stamm et al.'s JPEG anti-forensic method [2]. They borrowed the idea of calibration from steganalysis [8] for cropping image matrix X by 4 pixels both horizontally and vertically to obtain X_{cal}. The calibrated feature K_L is established as:

$$K_L = \frac{1}{28}\sum_{k=1}^{28}\left(\frac{v_{X,k} - v_{X_{cal},k}}{v_{X,k}}\right), \tag{6}$$

where $v_{X,k}$ and $v_{X_{cal},k}$ are the variances of the k-th high-frequency subband (defined in [5]) of X and X_{cal}, respectively.

3. JPEG DEBLOCKING USING CONSTRAINED TV-BASED MINIMIZATION

Some researchers have investigated the problem of removing JPEG blocking artifacts. However, their efforts mainly focused on improving image visual quality [9, 10, 11], especially for highly compressed images. Nevertheless, the objective of anti-forensics takes higher priority of statistical undetectability than perceptual quality. For JPEG anti-forensic deblocking purpose, we hereby propose to remove JPEG blocking artifacts using a variational approach minimizing a TV-based energy, which is composed of two terms: a TV term and a TV-based blocking measurement term.

Inspired by [10], which aims to improve the visual quality of images compressed at low bit-rates by solving a constrained and weighted TV-based minimization problem, for an image X of size $H \times W$, we first define the TV term as:

$$\text{TV}_b(X) = \sum_{1\le i\le H, 1\le j\le W} e_{i,j} \tag{7}$$

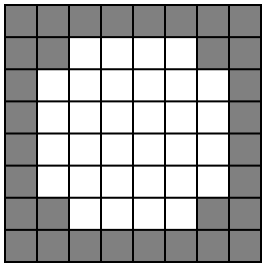

Fig. 1. Pixel classification according to its position in the block.

with the variation at location (i, j) as:

$$e_{i,j} = \sqrt{(x_{i-1,j} + x_{i+1,j} - 2x_{i,j})^2 + (x_{i,j-1} + x_{i,j+1} - 2x_{i,j})^2}. \tag{8}$$

In order to remove the statistical traces of JPEG blocking artifacts, we define a second term which measures the JPEG blocking. The idea is very simple: it assumes that if there is no compression, statistically the energy sum of the pixel value variation along the block borders should be close to that within the block. Hence, we divide all the pixels into two sets according to their positions in the block. The pixel classification strategy is illustrated in Fig. 1. For pixels whose positions are the same with the shaded cells, they are put into pixel set A, otherwise they are put into set B. Based on this, the second energy term is:

$$C(X) = \left| \sum_{x_{i,j}\in A} e_{i,j} - \sum_{x_{i,j}\in B} e_{i,j} \right|. \tag{9}$$

We also adopt a similar, yet less stringent constraint as that in [10] with the objective to achieve a good quality of the processed image. Given a quantization table Q of size 8×8, let $T : \mathbb{R}^{H\times W} \to \mathbb{R}^{H\times W}$ be the orthogonal linear block DCT transform that maps any image matrix X of size $H \times W$ to DCT coefficient matrix $T(X)$ with the same size. Denote U as the constraint space of images:

$$\begin{aligned} U = \{X \in \mathbb{R}^{H\times W} | \forall i = 1, \ldots, H, j = 1, \ldots, W, \\ (T(X))_{i,j} \in [(k_{i,j} - \frac{3}{2})Q_{(i-1)\%8+1,(j-1)\%8+1}, \\ (k_{i,j} + \frac{3}{2})Q_{(i-1)\%8+1,(j-1)\%8+1}]\}, \end{aligned} \tag{10}$$

where $\%$ is the modulo operator, and $k_{i,j}$ can be easily obtained from the JPEG image $\tilde{X}$ whose (i, j)-th DCT coefficient value $(T(\tilde{X}))_{i,j} = k_{i,j}Q_{(i-1)\%8+1,(j-1)\%8+1}$. We set this constraint space to ensure that the DCT coefficients of the processed image are within the same or the neighboring quantization bins as those of the JPEG image $\tilde{X}$.

The final constrained TV-based minimization problem is:

$$\begin{aligned} &\text{minimize} \quad E(X) = \text{TV}_b(X) + \lambda C(X) \\ &\text{subject to} \quad X \in U, \end{aligned} \tag{11}$$

where $\lambda > 0$ is a regularization parameter, balancing the two energy terms. $E(X)$ is a convex function and U is a convex set [10, 12]. The optimization problem can be solved using projected subgradient method [13] giving the solution:

$$X^* = P(X^* - t \times g(X^*)), \tag{12}$$

where $t > 0$ is the step size, and $g(X)$ is a subgradient of $E(X)$. Note that P is the projection operator onto U, which can be considered as a *relaxed* version of the classical quantization constraint set projection, that strictly constrains the processed DCT coefficient to stay in the same bin as its original value [10].

4. JPEG ARTIFACTS BEYOND BLOCKING

In practice, we found out that after our deblocking process described in Sec. 3, besides Fan and De Queiroz's blocking artifact detector [1], we also succeeded in fooling the TV-based detector of Valenzise et al. [4]. Meanwhile the calibrated feature value, *i.e.*, K_L of Eq. (6), has also been significantly decreased. However, for genuine, uncompressed images, this feature value is highly condensed in an interval of very small values. It is hard to further decrease this value by performing deblocking, while keeping good visual quality. In this section, as a first trial to defeat this detector, we will directly optimize an energy function which is very close to Eq. (6) for *de-calibration* purpose.

Denote $D = [d_1^T, \cdots, d_{64}^T]^T$ as the block DCT matrix in JPEG compression, where $d_i^T, i = 1, \cdots, 64$ is a 64×1 vector. We define a stacking operator $\text{stc}(\cdot)$, so that $S = \text{stc}(X)$ is a $64 \times \lfloor \frac{H \times W}{64} \rfloor$ matrix. Each column vector s_j of S is a column-wise stacking of the j-th 8×8 block in X. Thereafter, $d_i s_j$ is the i-th DCT coefficient of the j-th block in X after block DCT. And the row vector $d_i S$ contains all the DCT coefficients in the i-th subband.

Hence the minimization problem is formulized as:

$$X^* = \arg\min_X \sum_{k=1}^{28} |\text{var}(d_{i_k}\text{stc}(X)) - \text{var}(d_{i_k}\text{stc}(X_{cal}))|, \quad (13)$$

where d_{i_k} corresponds to the k-th high-frequency subband defined in [5], and $\text{var}(\cdot)$ returns the variance of the input vector. This problem can also be solved using subgradient method.

5. EXPERIMENTAL RESULTS

Our large-scale test was carried out on 1338 images of size 512×384 from the UCID corpus [14]. Without loss of generality, only the luminance component of the image is considered. Denote $\{\mathcal{I}_k | k = 1, 2, \cdots, 1338\}$ as the set of all the original uncompressed images in UCID. We compressed each UCID image at a quality factor[1] randomly selected in the interval of $[30, 90]$. Thereafter a set of JPEG compressed images $\{\mathcal{J}_k\}$ is generated. We also created five other image sets from $\{\mathcal{J}_k\}$ as follows:

- $\{\mathcal{F}_k^A\}$, with the application of Alter et al.'s deblocking method [10] on $\{\mathcal{J}_k\}$;
- $\{\mathcal{F}_k^{S_b}\}$, with the application of Stamm et al.'s deblocking method [3] on $\{\mathcal{J}_k\}$, with parameters $s = 3$ and $\sigma^2 = 2$, as suggested in [3];
- $\{\mathcal{F}_k^{S_q S_b}\}$, with Stamm et al.'s dithering signals [2] added on $\{\mathcal{J}_k\}$ first, and then Stamm et al.'s deblocking operation [3] was applied, with parameters $s = 3$ and $\sigma^2 = 2$;
- $\{\mathcal{F}_k^{F_b}\}$, with the application of our proposed deblocking operation described in Sec. 3 on $\{\mathcal{J}_k\}$;
- $\{\mathcal{F}_k^{F_b F_c}\}$, with the application of our proposed de-calibration operation described in Sec. 4 on $\{\mathcal{F}_k^{F_b}\}$.

In order to verify the undetectability of the proposed deblocking method, it is necessary to test against detectors using different blocking criteria [15]. Therefore, besides the blocking artifact detector in [1], we build another JPEG blocking signature measure:

$$K_U^p = |B_{gr}^p(X) - B_{gr}^p(X_{cal})|, \quad (14)$$

[1]All the JPEG compression and decompression operations in this paper were performed using *libjpeg* version 6b provided by Independent JPEG Group. More information can be found at `http://www.ijg.org/`.

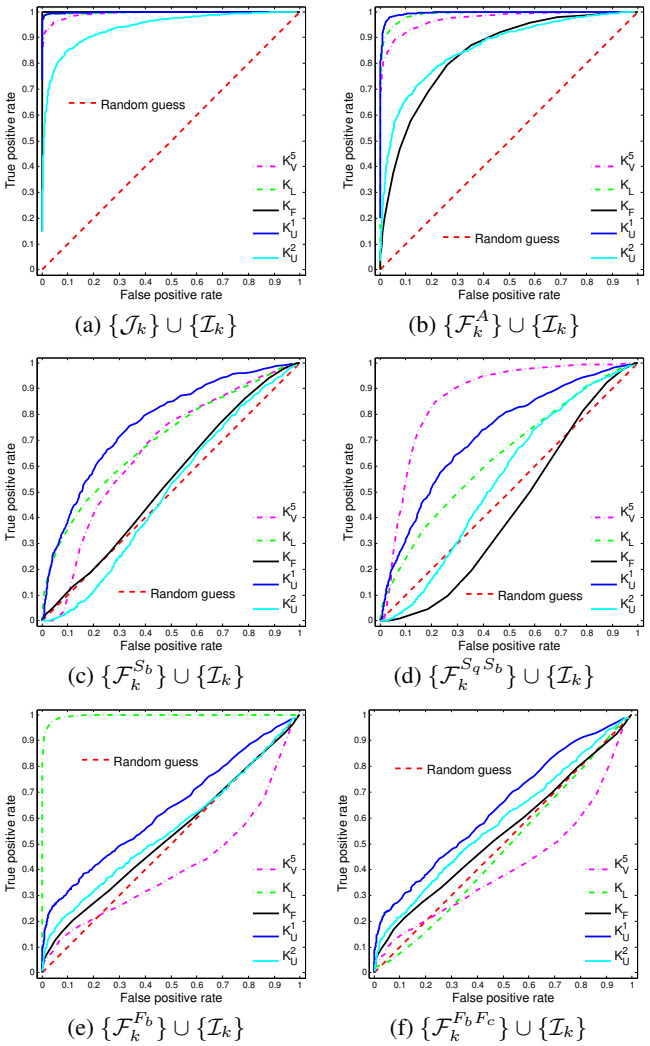

(a) $\{\mathcal{J}_k\} \cup \{\mathcal{I}_k\}$ (b) $\{\mathcal{F}_k^A\} \cup \{\mathcal{I}_k\}$

(c) $\{\mathcal{F}_k^{S_b}\} \cup \{\mathcal{I}_k\}$ (d) $\{\mathcal{F}_k^{S_q S_b}\} \cup \{\mathcal{I}_k\}$

(e) $\{\mathcal{F}_k^{F_b}\} \cup \{\mathcal{I}_k\}$ (f) $\{\mathcal{F}_k^{F_b F_c}\} \cup \{\mathcal{I}_k\}$

Fig. 2. ROC curves of different image sets under JPEG forensic detectors. The closer the curve is to *Random guess*, the better the detector is fooled.

where B_{gr}^p is the gradient aware blockiness [16], which is the normalized ℓ_p norm of the weighted gradient computed from each group of four adjacent pixel values across block borders.

In this paper, the detectors described in Sec. 2, together with the above blocking artifact detector, are used for the testing of forensic undetectability of the image sets. For the sake of simplicity, we name the detectors directly using the feature value name, that is K_V^h, K_L, K_F, and K_U^p in Eqs. (5), (6), (1), and (14) respectively. Here, we consider the parameters $h = 5$, $p = 1$, and $p = 2$. Figure 2 shows the ROC curves of different image sets against the detectors K_V^5, K_L, K_F, K_U^1, and K_U^2 respectively. The detection relability $\rho = 2a - 1$, where a is the area under the ROC curve [16], is reported in Table 1. The average PSNR and SSIM [17] values are provided in Table 2 for the comparison of the quality of processed images.

Apparently fooling detectors is not the goal of Alter et al.'s work [10], as their main focus is to improve the image perceptual quality[2].

[2]Note that in Table 2, the average PSNR and SSIM values of $\{\mathcal{F}_k^A\}$ are both lower than those of $\{\mathcal{J}_k\}$. The reason may be that the parameter setting in [10] is optimized for low bit-rate compression, but not for the whole quality factor range of $[30, 90]$.

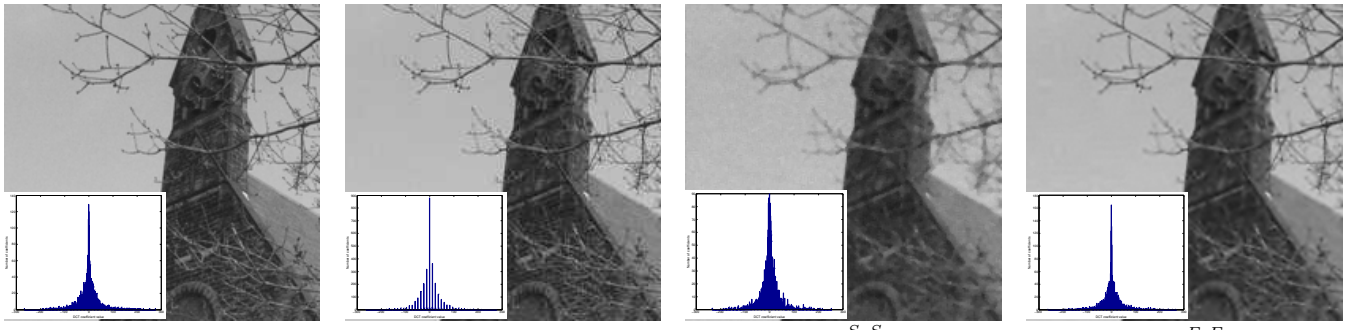

(a) $\mathcal{I}_{k_0}$ (b) $\mathcal{J}_{k_0}$ (c) $\mathcal{F}_{k_0}^{S_q S_b}$ (d) $\mathcal{F}_{k_0}^{F_b F_c}$

Fig. 3. Example results (close-up images) of the proposed method compared with Stamm et. al.'s methods [2, 3]. The original k_0-th image $\mathcal{I}_{k_0}$ in UCID corpus has been JPEG compressed with quality factor 50 to obtain $\mathcal{J}_{k_0}$. The small figures in the bottom left are the histograms of $(2, 2)$ DCT coefficients of the corresponding images.

Table 1. Detection relability.

	K_V^5	K_L	K_F	K_U^1	K_U^2
$\{\mathcal{J}_k\}$	0.9853	0.9925	0.9998	0.9964	0.8812
$\{\mathcal{F}_k^A\}$	0.9435	0.9764	0.6352	0.9901	0.7229
$\{\mathcal{F}_k^{S_b}\}$	0.2837	0.3057	−0.0106	0.5298	−0.0090
$\{\mathcal{F}_k^{S_q S_b}\}$	0.7163	0.1666	−0.2293	0.4430	0.0994
$\{\mathcal{F}_k^{F_b}\}$	−0.2264	0.9896	−0.0111	0.2579	0.1048
$\{\mathcal{F}_k^{F_b F_c}\}$	−0.2217	−0.1867	0.0031	0.2688	0.1609

Table 2. Comparison of image quality.

	$\{\mathcal{J}_k\}$	$\{\mathcal{F}_k^A\}$	$\{\mathcal{F}_k^{S_b}\}$	$\{\mathcal{F}_k^{S_q S_b}\}$	$\{\mathcal{F}_k^{F_b}\}$	$\{\mathcal{F}_k^{F_b F_c}\}$
PSNR	35.1355	34.1031	30.2676	29.8271	34.1186	34.0484
SSIM	0.9870	0.9820	0.9528	0.9407	0.9789	0.9785

Stamm et al.'s deblocking method [3] successfully fools blocking artifact detectors K_F and K_U^2, however K_U^1 still keeps a detection reliability value of around 0.5 for both $\{\mathcal{F}_k^{S_b}\}$ and $\{\mathcal{F}_k^{S_q S_b}\}$. And the noise introduced by the dithering signal [2] can still be detected by K_V^5 after the deblocking operation [3]. Moreover, as pointed out in [15], their deblocking attack has not been tested against median filtering forensic detectors.

As shown in Fig. 2-(e), the proposed deblocking method successfully fools all the three blocking artifact detectors, as well as the TV-based detector K_V^5, at the cost of slightly lower visual quality than the JPEG compressed images (Table 2). After the de-calibration process, the calibration-based detector K_L is also defeated, as shown in Fig. 2-(f); meanwhile we keep high undetectability against other detectors and a high level of image visual quality (Table 2). Compared to Stamm et al.'s methods [2, 3], our method achieves a better trade-off between undetectability and the visual quality of processed images: the average PSNR value has been improved by 4.2 dB.

Figure 3 shows the processed anti-forensic images from an example JPEG compressed image at quality factor 50. As expected, Fig. 3-(d) processed using our TV-based method better preserves the image details such as textures and edges than -(c). It can also be observed that even after the deblocking operation [3], the spatial-domain noise introduced by the dithering signal [2] can still be noticed at the smooth areas of the image, *e.g.*, the sky area in Fig. 3-(c) (please refer to the electronic version for a better visibility).

6. DISCUSSION AND CONCLUSION

The regularization parameter λ in Eq. (11) and the step size t in Eq. (12) are two parameters we can adjust. During the simulation, we set $\lambda = 1.5$, and $t = 1/k$ at the k-th iteration. This parameter setting works well for our JPEG anti-forensic purposes.

In order to converge to X^* in Eq. (12), one would like to run as many iterations as possible. However, we found that the iteration giving the best K_F, K_U^1, or K_U^2 values are not always in the convergence. This can be explained by the fact that we deblocked the image not in a way directly minimizing the blocking signature measures, as they have different blocking criteria. In practice, we run 50 iterations, and choose the one giving the smallest K_F value as the final result. This gives satisfying results against all the three blocking artifact detectors. Moreover, it is also able to fool another advanced detector K_V^5. The reason may be that the TV term of Eq. (7) suppresses the unnatural noises that can be detected by K_V^5.

For the de-calibration operation, as we directly minimize the feature value, we are capable of obtaining very small K_L values when converging to X^* in Eq. (13). In order to fool the detector, a random threshold for each image is drawn from the distribution of the calibrated feature values for genuine, uncompressed images, and the iteration stops once K_L value drops below it.

During our deblocking and de-calibration processes, we did not explicitly smooth the DCT coefficient histogram. However, in practice, we observe that the gaps in the DCT coefficient histogram were plausibly smoothed (example DCT histograms of $(2, 2)$ subband are shown in Fig. 3). We also used the MLE method [1], the targeted detector of Stamm et al.'s DCT histogram smoothing method in [2], to estimate the quantization table of the processed images $\{\mathcal{F}_k^{F_b F_c}\}$. None of estimates was correct, and a very high portion of 93.20% of the images had the estimated quantization table full of entries being either 1 or "undetermined". This is an interesting observation that deserves future investigation. In all, our JPEG anti-forensic images can be passed off as never compressed by testing under existing JPEG forensic detectors. However we are aware that there might still exist some artifacts which can be detected by more reliable detectors to be designed in the future.

Further research shall be devoted to advanced optimization methods for solving the minimization problems, to further investigation of the calibrated feature in order to avoid optimizing the feature value directly, and to explicitly smoothing the DCT coefficient histogram to better approximate the original distribution.

Another interesting point might be to apply our JPEG anti-forensics to counter the most recent forgery localization method of JPEG images [18, 19], and to compare the performance of our method with that of other advanced histogram-based anti-forensic methods, *e.g.*, [20].

7. REFERENCES

[1] Z. Fan and R. L. De Queiroz, "Identification of bitmap compression history: JPEG detection and quantizer estimation," *IEEE Trans. Image Process.*, vol. 12, no. 2, pp. 230–235, 2003.

[2] M. Stamm, S. Tjoa, W. S. Lin, and K. J. Ray Liu, "Anti-forensics of JPEG compression," in *Proc. IEEE Int. Conf. Acoust., Speech, and Signal Process.*, 2010, pp. 1694–1697.

[3] M. Stamm, S. Tjoa, W. S. Lin, and K. J. Ray Liu, "Undetectable image tampering through JPEG compression anti-forensics," in *Proc. IEEE Int. Conf. Image Process.*, 2010, pp. 2109–2112.

[4] G. Valenzise, V. Nobile, M. Tagliasacchi, and S. Tubaro, "Countering JPEG anti-forensics," in *Proc. IEEE Int. Conf. Image Process.*, 2011, pp. 1949–1952.

[5] S. Lai and R. Böhme, "Countering counter-forensics: the case of JPEG compression," in *Proc Int. Conf. on Information Hiding*, 2011, pp. 285–298.

[6] G. Valenzise, M. Tagliasacchi, and S. Tubaro, "The cost of JPEG compression anti-forensics," in *Proc. IEEE Int. Conf. Acoust., Speech, and Signal Process.*, 2011, pp. 1884–1887.

[7] L. I. Rudin, S. Osher, and E. Fatemi, "Nonlinear total variation based noise removal algorithms," *Phys. D: Nonlinear Phenomena*, vol. 60, no. 1-4, pp. 259–268, 1992.

[8] J. Fridrich, M. Goljan, and D. Hogea, "Steganalysis of JPEG images: Breaking the F5 algorithm," in *Proc. Int. Workshop on Information Hiding*, 2003, pp. 310–323.

[9] A. W.-C. Liew and H. Yan, "Blocking artifacts suppression in block-coded images using overcomplete wavelet representation," *IEEE Trans. Cir. and Sys. for Video Technol.*, vol. 14, no. 4, pp. 450–461, 2004.

[10] F. Alter, S. Durand, and J. Froment, "Adapted total variation for artifact free decompression of JPEG images," *J. Math. Imaging Vis.*, vol. 23, no. 2, pp. 199–211, 2005.

[11] G. Zhai, W. Zhang, X. Yang, W. Lin, and Y. Xu, "Efficient image deblocking based on postfiltering in shifted windows," *IEEE Trans. Cir. and Sys. for Video Technol.*, vol. 18, no. 1, pp. 122–126, 2008.

[12] S. Boyd and L. Vandenberghe, *Convex Optimization*, Cambridge University Press, New York, NY, USA, 2004.

[13] D. Bertsekas, *Nonlinear Programming*, Athena Scientific, Belmont, MA, USA, second edition, 1999.

[14] G. Schaefer and M. Stich, "UCID - An uncompressed colour image database," in *Proc. SPIE: Storage and Retrieval Methods and Applications for Multimedia*, 2004, vol. 5307, pp. 472–480.

[15] R. Böhme and M. Kirchner, "Counter-forensics: Attacking image forensics," in *Digital Image Forensics*, H. T. Sencar and N. Memon, Eds., pp. 327–366. Springer, New York, NY, USA, 2013.

[16] C. Ullerich and A. Westfeld, "Weaknesses of MB2," in *Proc. of Int. Workshop on Digital Watermarking*, 2008, pp. 127–142.

[17] Z. Wang, A. C. Bovik, H. R. Sheikh, and E. P. Simoncelli, "Imag quality assessment: From error visibility to structural similarity," *IEEE Trans. Image Process.*, vol. 13, no. 4, pp. 600–612, 2004.

[18] T. Bianchi, A. De Rosa, and A. Piva, "Improved DCT coefficient analysis for forgery localization in JPEG images," in *Proc. IEEE Int. Conf. Acoust., Speech, and Signal Process.*, 2011, pp. 2444–2447.

[19] T. Bianchi and A. Piva, "Image forgery localization via block-grained analysis of JPEG artifacts," *IEEE Trans. Information Forensics and Security*, vol. 7, no. 3, pp. 1003–1017, 2012.

[20] P. Comesaña-Alfaro and F. Pérez-González, "Optimal counterforensics for histogram-based forensics," in *Proc. IEEE Int. Conf. Acoust., Speech, and Signal Process.*, 2013.